

# Enhanced photodynamic efficacy of PLGA-encapsulated 5-ALA nanoparticles in mice bearing Ehrlich ascites carcinoma

Maryam N. Shaker · Heba S. Ramadan ·  
Moustafa M. Mohamed · Ahmed M. El khatib ·  
Gamal D. Roston

Received: 19 July 2013 / Accepted: 2 September 2013 / Published online: 17 September 2013  
© The Author(s) 2013. This article is published with open access at Springerlink.com

**Abstract** Nanoparticles (NPs) fabricated from the biodegradable copolymer poly(lactic-*co*-glycolic acid) (PLGA) were investigated as a drug delivery system to enhance the photodynamic efficacy of 5-aminolevulinic acid (5-ALA) in mice bearing Ehrlich ascites carcinoma. The PLGA-encapsulated 5-ALA NPs were prepared using binary organic solvent diffusion method and characterized in terms of shape and particle size. The *in vivo* photodynamic efficiency in Ehrlich ascites-bearing mice was studied. The obtained particles were uniform in size with spherical shape of mean size of 249.5 nm as obtained by particle size analyzer and the *in vitro* release studies demonstrated a controlled release profile of 5-ALA. Tumor-bearing mice injected with PLGA-encapsulated 5-ALA NPs exhibited significantly smaller mean tumor volume, increased tumor growth delay compared with the control group and the group injected with free 5-ALA during the time course of the experiment. Histopathological examination of tumor from mice treated with PLGA-encapsulated 5-ALA NPs showed regression of tumor cells, in contrast to those obtained from mice treated with free 5-ALA. The results indicate that PLGA-encapsulated 5-ALA NPs are a successful delivery system for improving photodynamic activity in the target tissue.

**Keywords** Photodynamic therapy (PDT) · Nanoparticles (NPs) · Photosensitizer (PS) · 5-Aminolevulinic acid

M. N. Shaker (✉) · A. M. El khatib · G. D. Roston  
Physics Department, Faculty of Science, Alexandria University,  
Alexandria, Egypt  
e-mail: maryam.nabil@alex-sci.edu.eg

H. S. Ramadan · M. M. Mohamed  
Biophysics Department, Medical Research Institute, Alexandria  
University, Alexandria, Egypt

(5-ALA) · Poly-lactide-*co*-glycolide (PLGA) · Percentage of drug entrapment (PDE) · Drug loading · Drug release

## Introduction

Photodynamic therapy also known as PDT, photo-radiation therapy, phototherapy, or photo chemotherapy is a promising treatment for a variety of oncological, cardiovascular, dermatological and ophthalmic diseases. PDT is emerging as an alternative modality for cancer therapy for the treatment of light accessible tumors (Saxena 2005).

Photodynamic therapy incorporates a photosensitizer (PS), light source, and oxygen. Individually, the components are nontoxic. The activated (irradiated) form of the photosensitizer is toxic at the site of action (Issa and Manela-Azulay 2010; Yoo et al. 2012). Among various photosensitizers, 5-aminolevulinic acid (5-ALA) is a precursor of a strong photosensitizing agent, protoporphyrin IX (PpIX) and has been used extensively in clinical applications, due to its safety, feasibility as an effective endogenous photosensitizer for fluorescence diagnosis, and its efficacy in PDT. However, owing to the poor penetration of ALA into skin, ALA-PDT is inappropriate for difficult-to-treat deep skin neoplasias (Donnelly et al. 2010). As most photosensitizers, 5-ALA is characterized by a high lipophilicity. Although interesting with respect to the selectivity for neoplastic tissue, the resulting insolubility in physiologically acceptable media makes the systemic administration of conventional PS problematic and restricts their medical applications (Castano et al. 2005; Konan et al. 2002). To overcome this limitation, PS have been associated with colloidal carriers such as liposomes, emulsions, microparticles or nanoparticles as reviewed by Konan et al. (2002). The interest in nanocarriers such as

polymeric nanoparticles (NPs) to enable the production of an injectable suspension of PS has been increasing over recent years. NPs made of a polymeric matrix are a very stable and biocompatible drug delivery system.

Polymeric NPs have the potential to dramatically improve the diagnosis and treatment of tumor (Lee et al. 2012; Qian et al. 2008). The ability to fine-tune the properties of nanoparticles by controlling their components in the core or the shell region renders them useful and optimal for pharmaceutical purposes (Lee et al. 2012; Ferrari 2005). Among them, Poly(D,L-lactide-co-glycolide) (PLGA) NPs have been demonstrated as excellent carriers for imaging and targeting of tumor cells and for carrying anti-tumor drugs to tumor cells, due to their unique features including biocompatibility, biodegradability, tailor-made functionality, and the large interior cargo volume (Lee et al. 2004, 2012; Zhang et al. 2007).

5-Aminolevulinic acid was simply conjugated to PLGA NPs for enhancing the nanoparticles stability in the PDT. The conjugation of 5-ALA to PLGA NPs was designed to perform photodynamic tumor therapy by generating reactive oxygen species (e.g., singlet oxygen:  $^1\text{O}_2$ ) from light absorption. The released reactive oxygen species lead to irreversible damage to the treated tumor cells (Oh et al. 2012; Park et al. 2011).

In this study, we prepared PLGA NPs by emulsion solvent evaporation method compared with the binary organic solvent diffusion (BOSD) method, and studied the possibility of nanoparticles as drug carriers by using 5-ALA as a model of photosensitizer drug. The drug loading contents, loading efficiency, changes of particle size, and physicochemical properties of PLGA NPs after the drug is entrapped into the nanoparticles are investigated. Also the use of laser and PLGA-encapsulated 5-ALA NPs as possible dual-mode enhancement agents in mice bearing Ehrlich ascites carcinoma is explored.

## Materials and methods

### Materials

Poly (D,L-lactide-co-glycolide) (PLGA, lactide/glycolide molar ratio = 85/15, average Mw 50,000–75,000), 5-aminolevulinic acid hydrochloride, poly (vinyl alcohol), 87–89 % hydrolyzed, average Mw 13,000–23,000 all those was provided by Sigma Chemical Co. USA, and all other chemicals and solvents were of reagent grade.

### PLGA nanoparticles preparation

PLGA NPs were prepared as follows.

### Spontaneous emulsification solvent diffusion (SESD)

Briefly, 60 mg of PLGA (85:15) were first dissolved in 25 mL of acetone; this organic phase was poured at the rate of 0.4 mL/min into 30 mL phosphate buffer (pH 7.4, 5 mM) containing 100 mg PVA as the hydrophilic surfactant under moderate magnetic stirring of 2,000 rpm. Finally, the organic solvents were evaporated under reduced pressure at 58 °C, and the final volume of the aqueous suspension was adjusted to 10 mL (Lamprecht 1999).

But this method resulted in nanoparticles of large mean size of about 233 nm.

### Binary organic solvent diffusion (BOSD) (Jiang et al. 2003)

1. 60 mg of PLGA (85:15) was first dissolved in 17 mL of acetone in a glass beaker then 8 mL of ethanol is added drop-wise using a 22-gauge micro-infusion syringe pump at rate of 0.4 mL/min into 30 mL double distilled water containing 100 mg PVA as the hydrophilic surfactant with stirring of 2,000 rpm with the help of a high-speed magnetic stirrer.
2. After addition of the organic solvent, the solution stirred on the high-speed magnetic stirrer for about one extra day.

### Purification

3. The organic solvents of acetone and ethanol were evaporated under reduced pressure at 58 °C using rotary evaporator and then centrifuged at 12,000 rpm for 1 h.
4. The precipitate was washed with 25 mL distilled water. This centrifugation and washing process was repeated three times to remove the PVA and residual organic solvents.

### Freeze-drying

5. The precipitate was frozen by vacuum freeze-drying machine (Lyophilizer) (Model/CRYODOS-50, Spain) at 230 V, 50 Hz, at a pressure of 26.5 Pa and 5 % saccharose was used as cytoprotectant. The lyophilized particles were then characterized.

### Characterization of PLGA nanoparticles

#### Particle size (Thakkar et al. 2004)

The particle size distribution of the nanoparticles was determined by laser light scattering on a Beckman Coulter Particle Size Analyzer (N5 submicron particle size

analyzer, Japan) equipped with a He–Ne Laser beam at a fixed scattering angle of 11.1°. The nanoparticles suspension were added to the sample dispersion unit containing the stirrer and stirred to reduce the aggregation between the particles, and laser obscuration range was maintained at 15–20 %. The mean particle size was measured after performing the experiment in triplicate.

#### *Shape of PLGA nanoparticles (Gupta and Jabrail 2006)*

The physical size and shape of the prepared nanoparticles were determined by transmission electron microscope (JEOL-JSM-6360LA, Japan). For this purpose, the particle suspension was diluted 10 times with distilled water and deposited drop-wise onto a 400-mesh copper grid coated with carbon film, and were allowed to dry in the air before studying by microscope.

#### *Fourier-transform infrared spectroscopy (FTIR) (Bhumkar and Pokharkar 2006)*

Fourier-transform infrared (FTIR) spectra of the blank PLGA NPs were obtained on a Shimadzu FTIR-8400S (Tokyo, Japan). The pellets were prepared by grinding 4–8 mg of samples with 200 mg potassium bromide and by a compression using Shimadzu compressor (Japan) tablets were prepared then fixed on holder to be examined. The spectra were scanned over the wave number range of 4,600–500 cm<sup>-1</sup> in which the region of 4,600–600 cm<sup>-1</sup> are called the functional group region.

#### *Thermo-gravimetric analysis (TGA) (Bhumkar and Pokharkar 2006)*

The compositions of the prepared nanoparticles were determined by thermo-gravimetric analysis (TGA) (TGA 50, Shimadzu, Japan). The weight of the dried nanoparticles for the TGA experiment was between 13 and 16 mg. The experiments were conducted using closed aluminum pans with a cover hole. The sample was examined under a nitrogen flow rate of 20 mL/min at a scan rate 10 °C/min with the range from 25 to 600 °C.

#### *Determination of encapsulation efficiency (Thakkar et al. 2004)*

The percentage of drug entrapment (PDE) was calculated according to Eq. (1) as following:

$$\text{PDE (\%)} = \frac{\text{Actual drug content}}{\text{Theoretical drug content}} \times 100 \% \quad (1)$$

*Theoretical drug content* was determined assuming that the entire drug present in the PLGA solution used gets entrapped in nanoparticles and no loss occurs.

*The actual drug content* in the 5-ALA loaded PLGA nanoparticles was quantitatively determined by the following procedure:

First standard curve from known concentration of 5-ALA was constructed. Freeze-dried nanoparticles were weighted and suspended into methanol and vigorously stirred for 3 h and sonicated for 15 min. Resulting solution was centrifuged at 12,000 rpm for 20 min. The supernatant was taken for measurement of drug concentration using ultraviolet (UV)/visible spectrophotometer (new Jenway Model 6315) at 670 nm. The drug loading efficiency (DLE) was presented by Eq. (2) (Nah et al. 2000).

$$\text{DLE} = \frac{\text{Weight of drug in nanoparticles}}{\text{Weight of nanoparticles}} \quad (2)$$

#### *In vitro drug release*

The in vitro drug release study was performed in triplicate. Briefly, 15 mg freeze-dried drug-loaded nanoparticles was suspended in 50 mL phosphate buffer saline (PBS), pH 7.4, in a glass flask and sonicated using Bransonic Ultrasonic B-220 for 10 min to get a homogenous suspension. This suspension was kept in shaking on a mechanical shaking bath shaken horizontally at 100 cycles/min, with temperature adjusted to 37 °C. At different time intervals, a sample volume of 1.5 mL was transferred and centrifuged at 10,000 rpm for 15 min. A quantity of 1 mL of the supernatant was taken for laser analysis at 670 nm. 1 mL of fresh PBS buffer was added to the remaining 0.5 mL sample. 1.5 mL of the suspension was agitated vigorously by vortexing and replaced in the flasks. The cumulative percentage of 5-ALA released from the nanoparticles at a certain time point was obtained using Eq. (3).

$$\begin{aligned} \text{Cumulative 5-ALA released \%} \\ = 100 - (5\text{-ALA remaining}) \% \end{aligned} \quad (3)$$

The same procedure was repeated where the sample were irradiated to a diode laser at 650 nm laser beam from a He–Ne laser (photon company) as measured by spectrometer, the power of each laser on the sample was 150 mW. During the experiments, the laser beam was delivered to the tubes containing samples with an irradiation spot of 7 mm diameter. The fluency rate was 3.90 mW/mm<sup>3</sup>. Laser irradiation lasted for 11 min, and then a sample volume of 1.5 mL was transferred and centrifuged at 10,000 rpm for 15 min. A quantity of 1 mL of the supernatant was taken for laser analysis at 670 nm. 1 mL of fresh PBS buffer was added to the remaining

0.5 mL sample. 1.5 mL of the suspension was agitated vigorously by vortexing and replaced in the flasks.

#### Animal care

In vivo studies were done on a total of 80 male Swiss albino mice 6–8 weeks old, weighing 16–25 g, purchased from animal house at National Cancer Institute, Cairo University. Ten animals each were housed in plastic cages in a well-ventilated room ( $25 \pm 2$  °C) with a relative humidity of ( $43 \pm 3$  %) and maintained on a high protein basal diet.

#### PDT protocol

Animals were acclimated to the environment for at least 2 weeks before onset of the experiment. Ehrlich ascites carcinoma cells,  $2 \times 10^6$  mammary in origin, diluted approximately (1–4) in 0.2 mL normal saline. The mouse's leg was shaved; the thigh skin was pulled up with forceps, and then inoculated subcutaneously.

The treatment protocol started with intralesional injection on the eighth day after tumor implantation. Animals were anesthetized with ketamine/xylazine/acepromazine and the dose of PLGA NPs administrated to each mouse was equivalent to 20 mg/kg which were suspended in saline and sonicated for 10 min before injection to get a homogenous suspension then directly injected into the tumor interstitial coordinates using insulin syringe. Within 2 min of injection to limit particle diffusion beyond the tumor boundaries, animal tumors were extra-corporeally exposed for 11 min to 670 nm visible diode laser at power of 150 mW (Casas et al. 1999) for each other day for 1 week (three times/week). During the experiment, laser beam was delivered to the tumor with an irradiation spot directly on the skin over the tumor of 7 mm diameter; fluency rate was  $3.90 \text{ mW/mm}^2$  at room temperature ( $25 \pm 2$  °C). During the procedure, a homemade thermo sensitive sensor connected to computer is to monitor the thermal transient of tumor and measure its temperature using a across a software interface the circuit of the sensor.

#### Experimental design

The animals injected with tumor cells were subdivided into four main groups each comprising 20 animals as follows:

*Group I* mice injected with free 5-ALA at dose of 20 mg/kg.

*Group II* mice injected with PLGA-encapsulated 5-ALA NPs at dose equivalent of 20 mg/kg.

*Group III* mice injected with blank PLGA NPs.

*Group IV* mice injected with 50  $\mu\text{L}$  normal saline and serve as the control untreated group.

Each group was divided into two subgroups each of 10 mice; subgroup A which did not receive laser irradiation. While subgroup B irradiated with laser beam for 11 min each other day (three times/week) for 1 week.

#### Inhibitory effect of 5-ALA loaded on nanospheres

To study the cytotoxic effect of 5-ALA loaded on PLGA nanospheres irradiated with laser on the tumor in different animal groups, the following parameters were estimated as follows.

#### Tumor volume

The tumor was measured every other day between the skin surface layers. Tumor volume was estimated using Eq. (4) as follows (Tang et al. 2007).

$$\text{Volume of tumor} = D_{\max} \times (D_{\min})^2 / 2. \quad (4)$$

where  $D_{\max}$  maximum diameter,  $D_{\min}$  minimum diameter

#### Tumor volume ratio (TVR) (Chen et al. 2004)

$$\text{TVR} = \frac{\text{Tumor volume after treatment}}{\text{tumor volume before treatment}} \quad (5)$$

#### Inhibition ratio of tumor (Tang et al. 2007)

$$\text{Inhibition ratio of tumor} = 1 - \left\{ \frac{\text{(average tumor volume at beginning - average tumor volume at the end of treatment)}}{\text{(average tumor volume of control at beginning - average tumor volume of control at the end of treatment)}} \right\} \quad (6)$$

#### Tumor growth relative rate (TGRR) (Venslauskas and Batiuskaite 2003)

The tumor growth at a given moment is dependent on the size of tumor cell population at the previous time interval and that the tumor growth rate at different time interval is not steady. On the other hand, under the influence of anticancer drug tumor growth could be stopped or reduced. These findings suggest proposing a new quantitative measure-tumor growth relative rate (TGRR) defined as:

$$r_t = (v_t - v_{(t-1)}) / \Delta t * (1/v_{(t-1)}) \quad (7)$$

where  $v_t$  is tumor volume at the present time interval,  $v_{(t-1)}$  is the tumor volume at the previous time interval,  $\Delta t$  is the time interval between the measurements so  $r_t$  is the

value of the tumor volume change per day expressed by part of the former volume.

### Biochemical analysis

Blood samples were collected when the mice were killed. Sera were harvested by centrifugation at 3,500 rpm and stored in aliquots at  $-80^{\circ}\text{C}$  until assayed. Serum TNF- $\alpha$  were determined using enzyme linked immunosorbent assay (ELISA) kit for the quantitative detection of TNF- $\alpha$  (eBioscience, Europe) according the producer's protocol.

### Histopathological study

**Light microscopic examination** On dissection, tumor samples were excised from animals of each group and preserved in a 10 % formalin solution for histopathological sections. The fixed tissues were embedded in paraffin; sections 3–5  $\mu\text{m}$  thick were obtained, deparaffinized, dehydrated in ethanol (50–100 %), and cleared with xylene. The extent of induced cytotoxicity, including inflammation, cell apoptosis, cell necrosis, steatosis and others was evaluated by assessing the morphological changes in tumor sections stained with hematoxylin and eosin (H&E) under light microscope. (Bancroft et al. 1996)

## Results and discussion

Characterization of blank PLGA and PLGA-encapsulated 5-ALA NPs

### Particle size

Figure 1a shows the particle size distribution curve, as measured by particle size analyzer, for blank PLGA NPs prepared by SESD method, sharp distribution range of nanoparticles, with 90 % of spheres in size range of 130–290 nm with mean size of 233.1 nm and only 10 % were oversized at diffraction angle of  $11.1^{\circ}$  with baseline

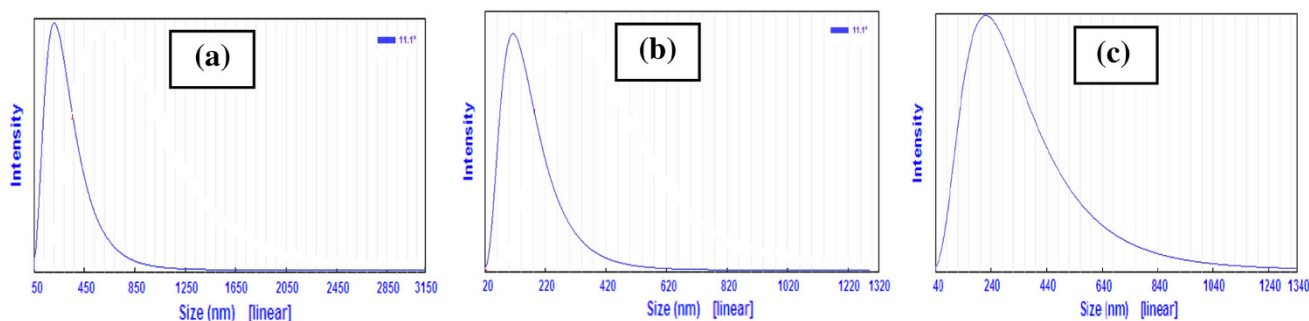
error of 0.01 % and poly-dispersity index of 0.856 ( $<1$ ) which indicates homogeneous distribution of the particles. These results were in accordance with Murakami et al's. (1999) study regarding production of PLGA NPs suggested that the original SESD method sometimes causes a severe aggregation in the particle formation process, resulting in formation of nanoparticles with larger size. This indicates that the SESD method should be modified. While Fig. 1b shows the particle size distribution curve for blank PLGA NPs prepared by BOSD method, sharp distribution range of nanoparticles, with 90 % of spheres in size range of 100–140 nm with mean size of 124.6 nm and only 10 % were oversized at diffraction angle of  $11.1^{\circ}$  with baseline error of 0.01 % and poly-dispersity index of 0.784 which also indicates homogeneous distribution of the particles. The binary organic solvents used were acetone and ethanol at the volume fraction of (2/1). The sizes of PLGA (85:15) NPs changes from 233 to 124 nm. Since ethanol has larger affinity to water than acetone and accelerates the diffusion of PLGA during dispersion process. This benefits the fast formation of NPs and avoids the aggregation of small particles, which results in the production of NPs with larger size (Wu et al. 2011).

Figure 1c shows the particle size distribution curve for PLGA-encapsulated 5-ALA NPs, it shows distribution range of nanoparticles, with 90 % of spheres in size range of 160–360 nm with mean size of 249.5 nm and only 10 % were oversized at diffraction angle of  $11.1^{\circ}$  with baseline error of 0.02 % and poly-dispersity index of 18.480 (more than 1) which indicates inhomogeneous distribution of the particles. Here, the increase in size is due to the addition of 5-ALA in NPs.

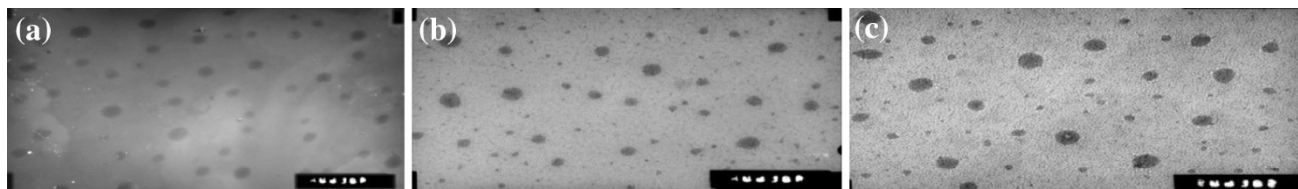
### Transmission electron microscope (TEM)

Figure 2a shows TEM examination for PLGA NPs prepared by SESD method; it revealed the presence of completely spherical PLGA NPs with smooth surfaces, and no agglomeration formed.

While Fig. 2b shows TEM examination for blank PLGA NPs prepared by BOSD method, it revealed the presence of

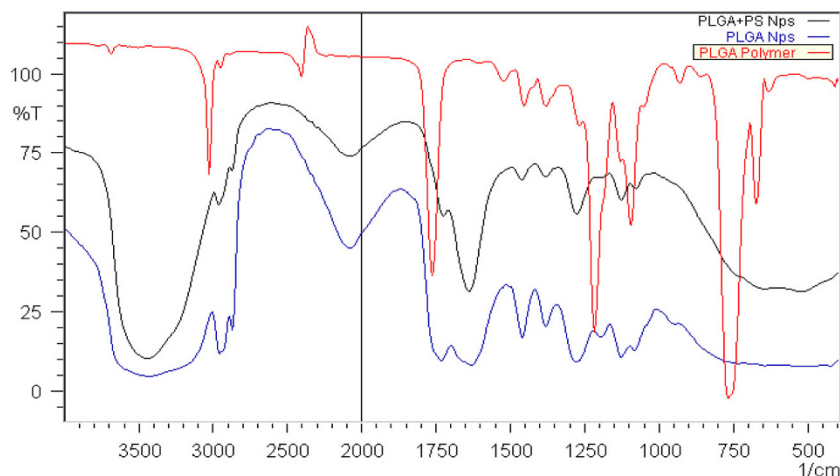


**Fig. 1** The particle size distribution curve for **a** free PLGA NPs prepared by SESD method. **b** Free PLGA NPs prepared by BOSD method. **c** PLGA-encapsulated 5-ALA NPs prepared by BOSD method



**Fig. 2** TEM of **a** blank PLGA NPs prepared by SEDS. **b** Blank PLGA NPs prepared by (BOSD). **c** TEM of PLGA-encapsulated 5-ALA NPs. All in  $\times 40$

**Fig. 3** Fourier-transform infrared spectra of PLGA polymer, blank PLGA NPs and PLGA-encapsulated 5-ALA NPs



completely spherical PLGA NPs with low level of agglomeration or adhesion that occurred among particles and high level of uniformity. But for PLGA-encapsulated 5-ALA NPs, Fig. 2c showed increased in size compared to free PLGA NPs and no change in the spherical shape which mean that the spherical shape of blank PLGA NPs has not been compromised.

#### Fourier-transform infrared spectroscopy (FTIR)

For the IR spectrum of PLGA polymer, the characteristic absorption bands appeared at wave number 3,023 and 2,401  $\text{cm}^{-1}$  (CH bend), 1,759  $\text{cm}^{-1}$  (C=O ester), 1,520, 1,451, 1,378  $\text{cm}^{-1}$  ( $\text{CH}_3$ ), 1,215, 1,126, 1,093  $\text{cm}^{-1}$  (C–O stretch), 748, 671  $\text{cm}^{-1}$  (CH– bend) while the band at 4,214 and 3,685  $\text{cm}^{-1}$  belongs to the OH group of the water molecule. While for blank PLGA NPs stabilized by PVA, it shows the characteristic absorption bands at wave number 3,423  $\text{cm}^{-1}$  (OH group), 2,954  $\text{cm}^{-1}$  (CH alkyl group), 2,866, 2,075  $\text{cm}^{-1}$  (CH bend), 1,730  $\text{cm}^{-1}$  (C=O ester), 1,631, 1,456, 1,379  $\text{cm}^{-1}$  ( $\text{CH}_3$ ), 1,276, 1,195, 1,126  $\text{cm}^{-1}$  (C–O stretch), 1,080  $\text{cm}^{-1}$  ( $\text{CH}_2$ ), 945, 732  $\text{cm}^{-1}$  (CH– bend). Also for PLGA-encapsulated 5-ALA NPs, it shows the same characteristic absorption bands at 3,438, 2,960, 2,867, 2,071, 1,724, 1,635, 1,458, 1,379, 1,274, 1,197, 1,126, 1,078, 642, 520  $\text{cm}^{-1}$ , in addition to a new band at 1,033  $\text{cm}^{-1}$  that C–O bond.

Comparing the obtained IR spectra for PLGA polymer, blank PLGA NPs and PLGA-encapsulated 5-ALA NPs as in Fig. 3 with the IR spectra characteristic for PLGA, PVA and 5-ALA shown in the literature, it confirmed that the obtained NPs are composed of PLGA and PVA with no interaction with 5-ALA. It was confirmed that there are no major shifting as well as no loss of functional peaks between the spectra of drug, polymer and drug-loaded NPs (3,438, 2,960, 2,867, 2,071, 1,724, 1,635, 1,458, 1,379, 1,274, 1,197, 1,126, 1,078, 642, 520  $\text{cm}^{-1}$ ). Besides the characteristic groups for PLGA, the large bands observed between 3,550 and 3,200  $\text{cm}^{-1}$  are linked to the stretching O–H from the intermolecular and intramolecular hydrogen bonds. The vibrational band observed between 2,840 and 3,000  $\text{cm}^{-1}$  refers to the stretching C–H from alkyl groups and the peaks between 1,750 and 1,735  $\text{cm}^{-1}$  are due to the stretching C–O and C–O from acetate group remaining from PVA (Mansur et al. 2008; Andrade et al. 2008).

Our results coincide with the results obtained by dos Reis et al. Their results indicated that FTIR spectrum of pure PVA sample clearly reveals the major peaks associated with poly(vinyl alcohol) that can be observed C–H broad alkyl stretching band ( $\nu = 2,850\text{--}3,000 \text{ cm}^{-1}$ ) and typical strong hydroxyl bands for free alcohol (nonbonded–OH stretching band at  $\nu = 3,600\text{--}3,650 \text{ cm}^{-1}$ ), and hydrogen bonded band ( $\nu = 3,200\text{--}3,570 \text{ cm}^{-1}$ ) (Budhian et al. 2007; Jain 2000). Intramolecular and intermolecular

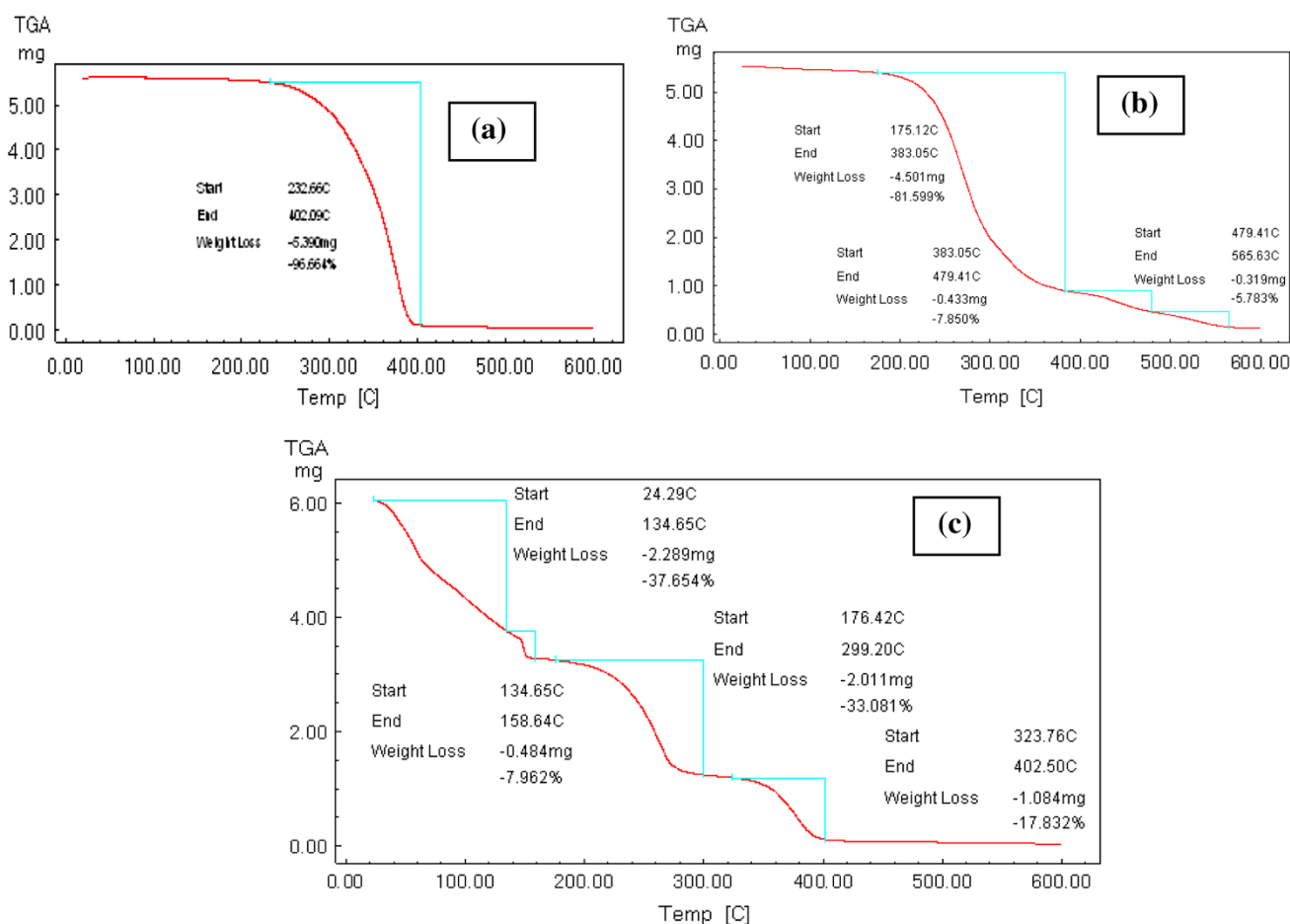


**Fig. 4** TGA of **a** PLGA powders. **b** Blank PLGA NPs. **c** PLGA-encapsulated 5-ALA NPs

hydrogen bonding are expected to occur among PVA chains due to high hydrophilic forces. An important absorption peak was verified at  $\nu = 1,142 \text{ cm}^{-1}$ . This band has been used as an assessment tool of PVA structure because it is a semi-crystalline synthetic polymer able to form some domains depending on several process parameters (John Coates and Meyers 2000; Elizabeth Fonseca dos Reis et al. 2006).

Our results are in agreement with the results obtained by Jawahar et al. They designed PLGA NPs for ramipril as anti-hypertensive agent confirmed no loss of functional groups of PLGA when processed into NPs loaded with ramipril (1,652, 1,701, 1,743, 2,866, 1,323  $\text{cm}^{-1}$ ) (Jawahar et al. 2009).

#### Thermo-gravimetric analysis (TGA)

Figure 4a shows TGA for PLGA powder which shows only one strong peak at 232–402 °C with 96.66 % loss of weight.

While Fig. 4b shows TGA for free PLGA NPs which shows three peaks, the larger one at 175–383 °C with

81.599 % loss of weight, next by shorter peak at 383–479 °C with 7.85 % loss of weight and the shortest peak at 479–566 °C with 5.783 % loss of weight.

While Fig. 4c shows TGA for PLGA-encapsulated 5-ALA NPs which shows four intermediate peaks at 24–135 °C with 37.654 % loss of weight, next by a very short peak at 135–159 °C with 7.962 % loss of weight and return to a stronger peak at 176–299 °C with 33.081 % loss of weight and ended by an intermediate peak at 324–402.5 °C with 17.832 % loss of weight.

#### Characterization of drug loading

According to Eqs. 1 and 2, PDE was 66.8 %, while DLE was 12.74 %. The drug load was 127.5  $\mu\text{g}$  drug/mg nanoparticles for PLGA NPs containing 5-ALA as shown in Table 1.

These results confirm the result of Jawahar et al. They prepared PLGA NPs containing ramipril a hypertensive agent with high PDE of 68.28 % (2009), while Budhian et al. (2008) prepared PLGA NPs (200 nm) encapsulating hydrophilic drug haloperidol with drug content of 0.2 %.

**Table 1** PDE and DLE for PLGA-encapsulated 5-ALA NPs

PLGA concentration (mg)	Initial concentration of 5-ALA (mg)	Encapsulated concentration of 5-ALA (mg)
26	5	3.34
PDE %	66.8 %	
DLE %	12.74 %	

The high 5-ALA incorporation efficiency in PLGA can be attributed to several factors:

Firstly, the hydrophobic nature of PLGA molecules makes it relatively easy to entrap hydrophobic 5-ALA into PLGA NPs.

Secondly, the hydrophobic nature of 5-ALA results in a minimum loss of the drug to the external aqueous phase during the interfacial deposition preparation process.

The high entrapment efficiency proves that the affinity between 5-ALA and PLGA matrix was far stronger than the affinity between 5-ALA and external aqueous phase.

Thirdly, the drug incorporation method and variables such as, incubation time, temperature, stirring, solvent, presence of surfactants, MW of PLGA, L:G ratio of PLGA, PLGA concentration, removal rate of organic solvent, etc., are also factors which may influence drug entrapment efficiency (Kader et al. 1998) and this in accordance with the explanation of Zeng and Sun (2009).

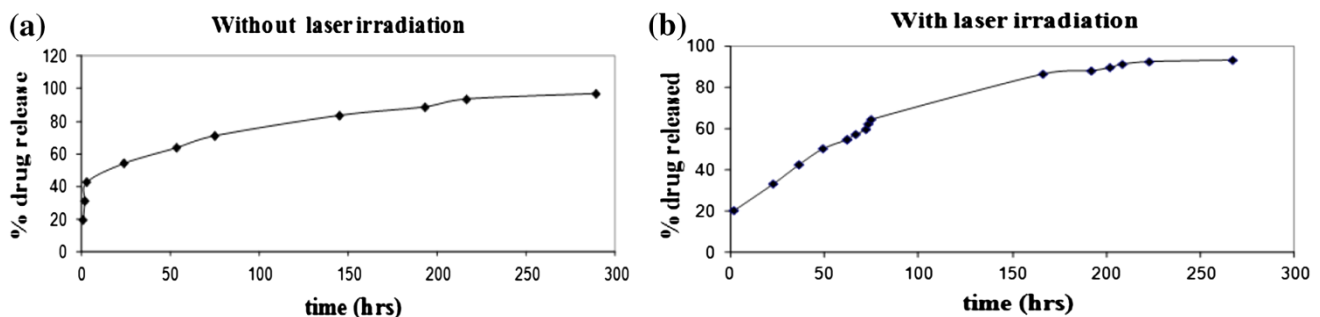
Figure 5a showed initial burst release profile of 54 % of 5-ALA from PLGA NPs after 24 h followed by a slower release rate that lasts for 12 days; this biphasic pattern is characterized by initial burst release followed

by a slow and continuous release rate as shown in the figure. This pattern of release is still the same even after laser irradiation at power intensity of  $150 \text{ mW/cm}^2$  for 11 min as in Fig. 5b which shows the initial fast release of 5-ALA was probably due to 5-ALA, which was adsorbed or close to the surface of the nanoparticles and diffused out of the nanoparticles into the released medium. The large surface-to-volume ratio of the nanoparticles geometry can be the contributing factor for the initial fast release pattern. The slow release of 5-ALA can be attributed to the diffusion of 5-ALA entrapped in the core of the nanoparticles into the aqueous media surrounding the nanoparticles. The release pattern observed in our study has been similar to those reported by Zeng and Sun (2009).

#### In vivo study

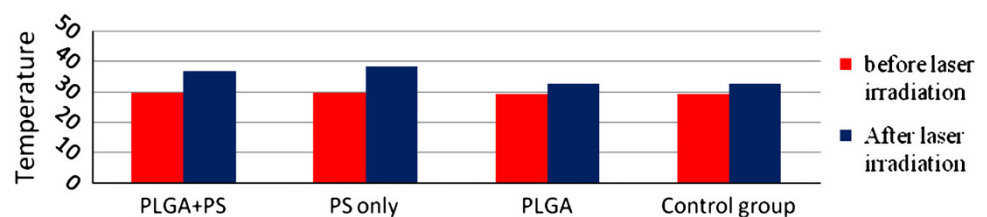
#### Temperature monitoring

At time of laser irradiation, all subgroups were monitored for temperature which revealed an increase in temperature of all subgroups compared with that before laser irradiation. While temperature in the subgroups that were injected with free 5-ALA and PLGA-encapsulated 5-ALA NPs increased significantly compared with the control group and the subgroup injected with blank PLGA NPs after laser irradiation (Fig. 6). This increased temperature confirmed by a necrosis occurs in the mice which was irradiated by laser and had taken free 5-ALA than that is not irradiated with laser where necrosis was found on histological examination of sections from each tumor. The areas of



**Fig. 5** Pattern of drug release of 5-ALA from PLGA NPs **a** without laser irradiation, **b** with laser beam for 11 min of power intensity  $150 \text{ mW/cm}^2$  as a function of time

**Fig. 6** Temperature change in the subgroups before and after irradiation with laser beam at  $670 \text{ nm}$  ( $150 \text{ mW/cm}^2$ ) for 11 min





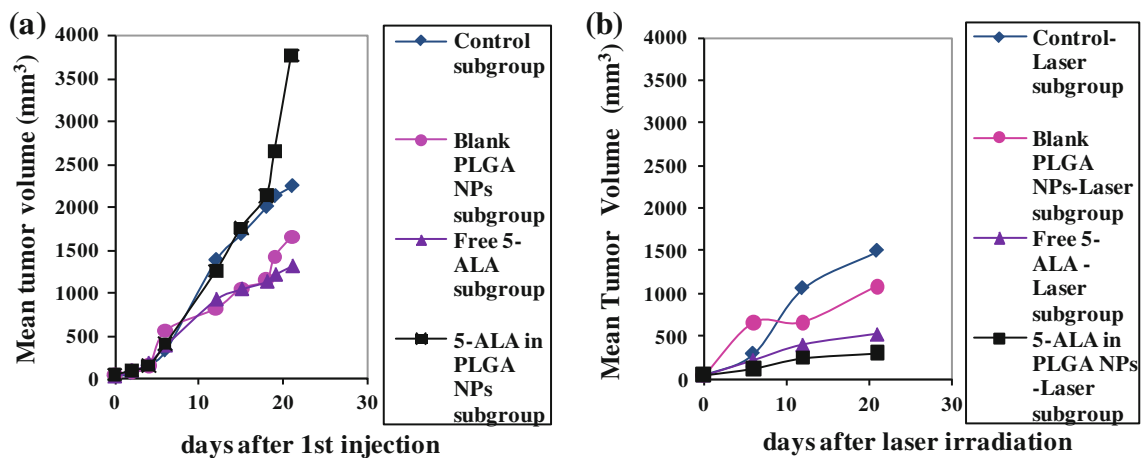


**Fig. 7** Tumor growth curves for the studied subgroups **a** without laser irradiation. **b** With laser irradiation at 670 nm ( $150 \text{ mW/cm}^2$ ) for 11 min

necrosis in irradiated tumors were larger (higher rank) than areas of necrosis of non-irradiated tumors (Egger et al. 1997).

#### Tumor growth and growth rate

All tumor volumes were normalized to that at the first day of treatment. All the four studied subgroups that were not irradiated with laser showed rapid tumor growth as shown in Fig. 7a. Mice bearing Ehrlich ascites carcinoma injected with free 5-ALA and irradiated with laser beam for 11 min showed reduced tumor volume compared to mice injected saline (control group) Fig. 7b. A severe decrease in tumor volume were seen in the subgroup of mice bearing Ehrlich ascites carcinoma, injected with PLGA-encapsulated 5-ALA NPs and irradiated with laser beam Fig. 7b. These results are in accordance with the results obtained by Lee et al. (2012) and Fadel et al. (2010). They formulated nanoparticles from the biodegradable copolymer poly (lactic-co glycolic acid) (PLGA) for targeting of zinc (II) phthalocyanine (ZnPc) for PDT in Ehrlich ascites carcinoma bearing mice. Tumor-bearing mice injected with ZnPc NPs exhibited significantly smaller mean tumor volume, increased tumor growth delay when compared with the control group and the group injected with free ZnPc during the time course of the experiment. Histopathological examination of tumor from animals treated with PLGA-ZnPc showed regression of tumor cells, in contrast to those obtained from animals treated with free ZnPc (Fadel et al. 2010).

#### Tumor growth inhibition

No significant difference in tumor volume was found among subgroups before treatment. For all the studied subgroups with no laser irradiation, the tumor grew rapidly

**Table 2** Tumor volume, tumor volume ratio (TVR) and inhibition ratio of tumor after treatment without laser irradiation

	Control	Blank PLGA	Free 5-ALA	5-ALA PLGA NPs
Tumor volume ( $\text{mm}^3$ )				
Before treatment	36.73	45.22	33.47	46.57
After 21 days of treatment	2,240.32	1,655.258	1,311.954	3,767.16
Tumor volume ratio (TVR)	60.99	36.60	39.19	80.89
Inhibition ratio of tumor after treatment (%)		26.9	42	−68

in mice of the control group, in which the mean tumor volume after 21 days was 60.99 times greater than that at the beginning as seen in Table 2.

For subgroups irradiated with laser beam, the tumor grew rapidly in mice of the control group, in which the mean tumor volume after 21 days was 39.72 times greater than that at the beginning as shown in Table 3. In contrast, tumor growth was less in volume in mice injected with free 5-ALA and PLGA-encapsulated 5-ALA NPs. The group treated with PLGA-encapsulated 5-ALA NPs showed a

**Table 3** Tumor volume, tumor volume ratio (TVR) and inhibition ratio of tumor after treatment in the presence of laser irradiation

	Control	Blank PLGA	Free 5-ALA	5-ALA PLGA NPs
Tumor volume ( $\text{mm}^3$ )				
Before treatment	37.58	39.75	44.21	45.74
After 21 days of treatment	1,492.92	1,082.7	530.76	302.3
Tumor volume ratio (TVR)	39.72	27.24	12	6.61
Inhibition ratio of tumor after treatment (%)		28.33	66.6	82.4

**Fig. 8** Mean tumor volume for all studied subgroups in the absence and presence of laser irradiation. **a** After 6 days of treatment. **b** After 12 days. **c** After 21 days

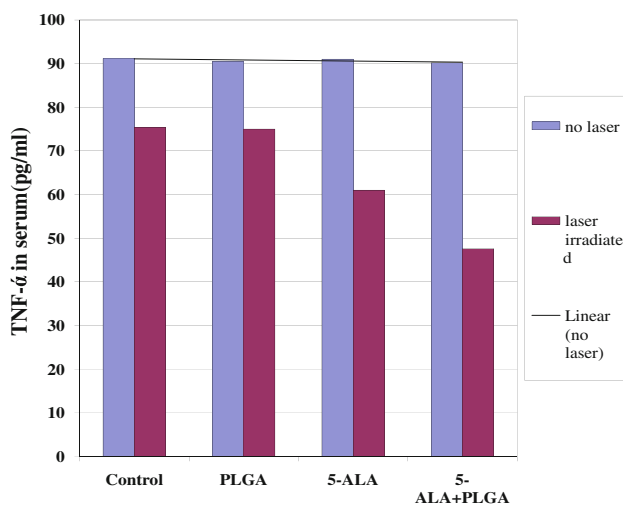
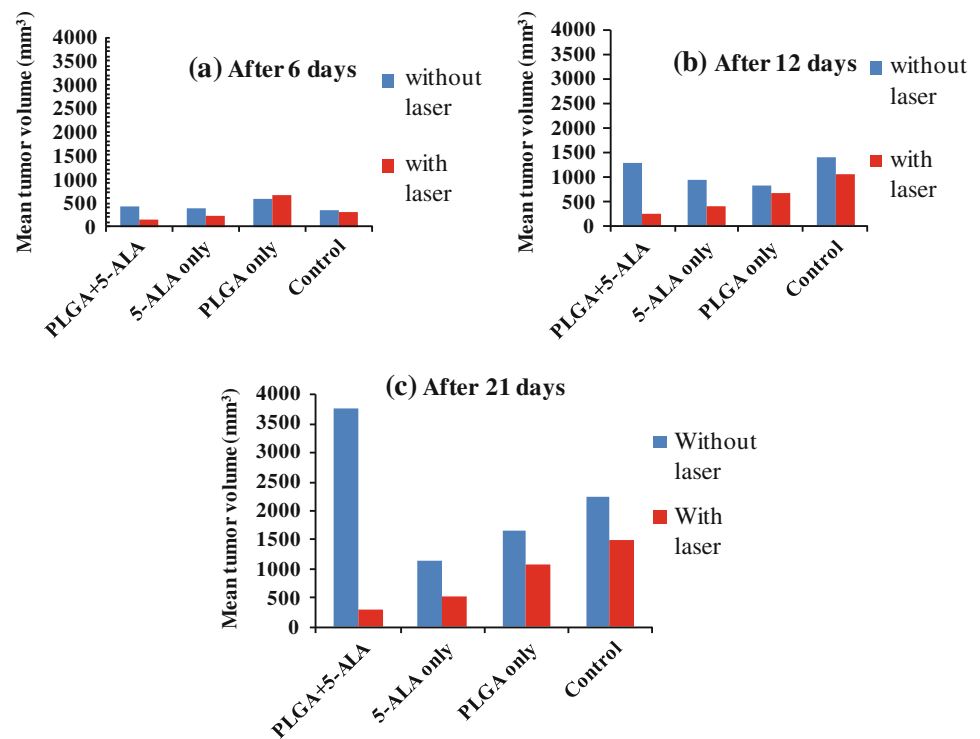


**Fig. 9** Biochemical analysis by TNF- $\alpha$  in blood serum for all subgroups with and without laser irradiation

statistical significance difference in tumor volume compared to that treated with blank PLGA NPs and also with free 5-ALA as shown in Fig. 8.

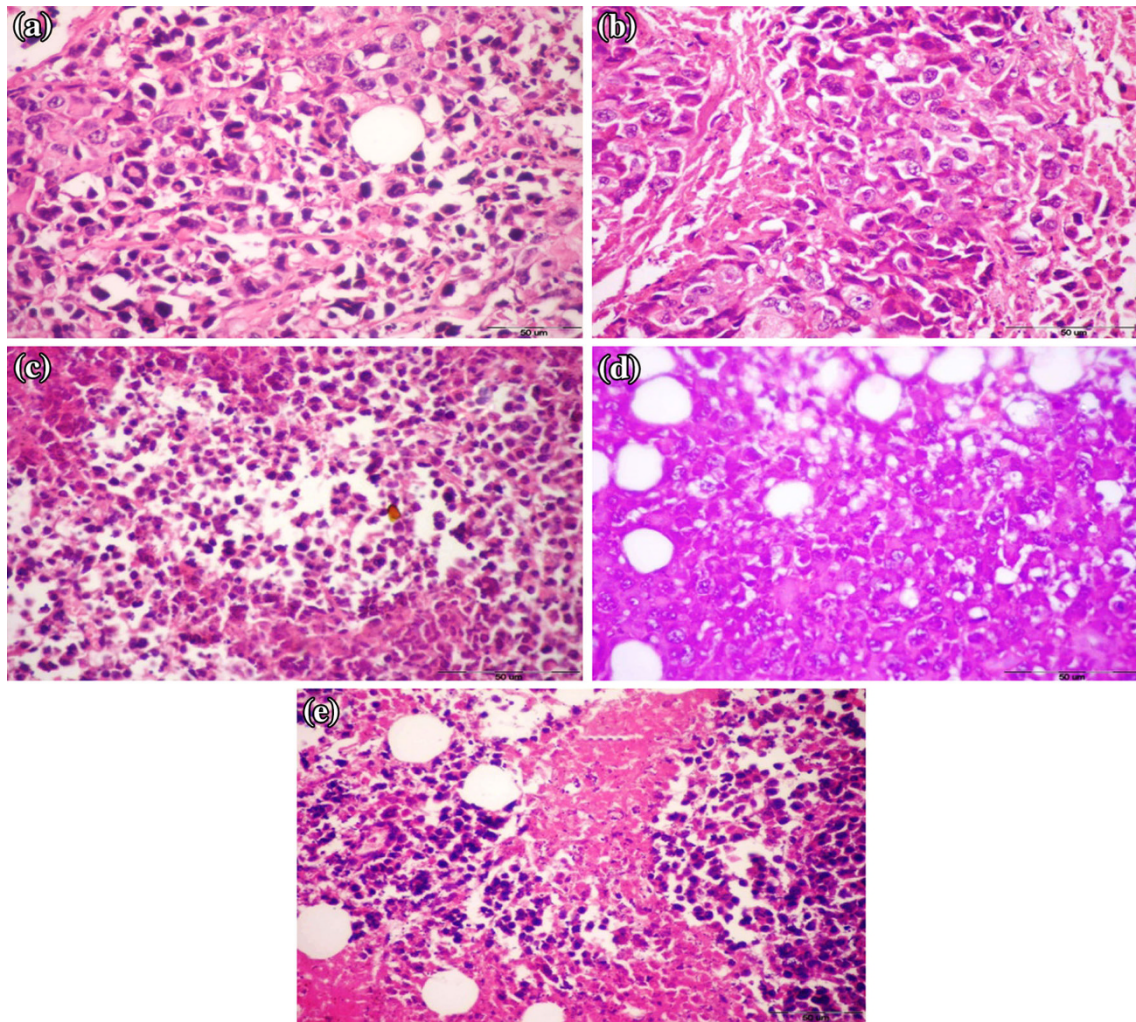
#### Biochemical analysis

Figure 9 shows the mean serum levels of TNF- $\alpha$  in mice bearing Ehrlich ascites carcinoma with no laser irradiation were non-significantly changed ( $P = 0.115$ ). While those injected with free 5-ALA and PLGA-encapsulated 5-ALA NPs and irradiated with laser showed significant reduction

of serum levels of TNF- $\alpha$  ( $P = 0.00$ ) compared with those injected with saline or blank PLGA NPs and irradiated with laser. These results confirmed the presence of necrosis and/or apoptosis which is confirmed by histopathological examination.

#### Macroscopic analysis and histological studies of paraffin section micrograph

Subgroups not treated with laser shows entirely viable tumors formed of sheets of polymorphic hyperchromatic malignant cells with bizarre giant forms and no evidence of necrosis was identified as in Fig. 10a, but tumor begins to be enhanced by exposing to laser beam 11 min 3 times per week for 1 week as it shows an increase number of large cells with visculated nuclei, reduction of multinucleate cell and no infiltrating lymphocytes cells Fig. 10b. For subgroups injected with PLGA NPs and irradiated to laser, it shows increase number of apoptotic cells characterized as pycnotic nuclei with basophilic cytoplasm other with hallo of vacuolated cytoplasm (Fig. 10c). For subgroups injected with 5-ALA only and irradiated with laser, it shows increase number of apoptotic cells regenerative cells characterized by vesicular nuclei and basophilic cytoplasm cells normal blood vessel large necrotic areas as shown in Fig. 10d. But for subgroup injected with PLGA-encapsulated 5-ALA NPs and irradiated with laser exhibited an improved in vivo PDT for the tumor site where it shows foci area of apoptotic cells surrounded by area of necrosis



**Fig. 10** Paraffin section micrograph for subgroups of Ehrlich ascites carcinoma **a** untreated. **b** Irradiated with laser beam. **c** Injected with free PLGA NPs and exposed to laser. **d** Injected free photosensitizer

(5-ALA) and exposed to laser. **e** Injected PLGA-encapsulated 5-ALA NPs and exposed to laser

and regenerative eosinophilic cytoplasm cells with vacuolated nuclei (Fig. 10e).

The administration of PLGA NPs resulted in a significant growth inhibition of the KB tumor bearing nude mice injected only once with PLGA NPs encapsulating chlorine e6 (Ce6) (a commonly used photosensitizer) or free Ce6 where 24 h post-injection, tumor sites were locally illuminated at a light intensity of  $5.2 \text{ mW/cm}^2$  using a 670 nm laser source for 40 min. The tumor volume in the nude mice treated with PLGA NPs was approximately 1.5 or 3 times smaller than those treated with free Ce6 or PBS (control). When compared to high-dose administration of free Ce6 (2.5 mg/kg), low-dose administration of NP1 NPs (equivalent Ce6 0.5 mg/kg body) were found to be more efficient for tumor regression (Lee et al. 2012). Also our results coincide with the results obtained by Fadel et al. (2010).

## Conclusion

As well as this study reports that entirely spherical shaped PLGA nanospheres of (124 nm) mean size were efficiently prepared by BOSD method rather than Spontaneous Emulsification Diffusion (SESD) method, also the resultant PLGA NPs allowed structural stability upon photosensitizer loading expressed in the volumetric expansion indicated by the increase in the mean particle size from empty NPs to 5-ALA loaded ones. 5-ALA as a model of photosensitizer was loaded to PLGA NPs with no deviation in FTIR and TGA pattern in reference to PLGA polymer. 5-ALA showed bimodal release pattern from PLGA NPs which is not affected by laser irradiation. This work nominates PLGA-encapsulated 5-ALA NPs for in vivo application of PDT studies, strongly supporting that laser-irradiated PLGA-encapsulated 5-ALA NPs 5-ALA can

effectively improve tumor PDT treatment options in terms of tumor volume reduction, growth regression and histopathology. We expect PLGA NPs to be tailor-made customizable for the desired functionality advancing the efficiency of anti-tumor management. So the feasibility of drug-encapsulated nanoparticles systems has been demonstrated and the advantages of such implanted systems are well known and include mainly: (1) minimizing systemic effects; (2) protecting the encapsulated drug from the physiologic medium; (3) obtaining high and sustained concentrations of the drug at the tumor site the particle chosen in this study was nanospheres. Indeed, if the particles are small enough, then they can be injected either through a needle into a discreet and functional area of the tissue or directly into a tumor that cannot be restricted because its location in turn will increase efficacy of PLGA-encapsulated 5-ALA nanoparticles in mice bearing Ehrlich ascites carcinoma.

**Open Access** This article is distributed under the terms of the Creative Commons Attribution License which permits any use, distribution, and reproduction in any medium, provided the original author(s) and the source are credited.

## References

- Andrade G, Barbosa-Stancioli EF, Mansur AA, Vasconcelos W, Mansur HS (2008) Small-angle X-ray scattering and FTIR characterization of nanostructured poly (vinyl alcohol)/silicate hybrids for immunoassay applications. *J Mater Sci* 43:450–463
- Bancroft JD, Stevens A, Tuener DR (1996) Theory and practice of histopathological techniques, 4th edn. Churchill Livingstone, Edinburgh
- Bhumkar DR, Pokharkar VB (2006) Studies on effect of pH on cross-linking of Chitosan with sodium tripolyphosphate: a technical note. *AAPS PharmSciTech* 7(2):Article 50
- Budhian A, Siegel SJ, Winey KI (2007) Haloperidol-loaded PLGA nanoparticles: systematic study of particle size and drug content. *Int J Pharm* 336:367–375
- Budhian A, Siegel SJ, Winey KI (2008) Controlling the in vitro release profiles for a system of haloperidol-loaded PLGA nanoparticles. *Int J Pharm* 346(1–2):151–159
- Casas A, Fukuda H, Meiss R, Battle AM (1999) Topical and intratumoral photodynamic therapy with 5-aminolevulinic acid in a subcutaneous murine mammary adenocarcinoma. *Cancer Lett* 141(1–2):29–38
- Castano AP, Demidova TN, Hamblin MR (2005) Mechanisms in photodynamic therapy: part three-photosensitizer pharmacokinetics, biodistribution, tumor localization and modes of tumor destruction. *Photodiagn Photodyn Ther* 2:91–106
- Chen J, Ling R, Yao Q, Wang L, Ma Z, Li Y, Wang Z, Xu H (2004) Enhanced antitumor efficacy on hepatoma-bearing rats with adriamycin-loaded nanoparticles administered into hepatic artery. *World J Gastroenterol* 10:1989–1991
- Coates J, Meyers RA (eds) (2000) Interpretation of infrared spectra, a practical approach. *Encyclopedia of Analytical Chemistry*. Wiley, Chichester, pp 10815–10837
- Donnelly RF, Morrow DI, Fay F, Scott CJ, Abdelghany S, Singh RR, Garland MJ, Woolfson AD (2010) Microneedle-mediated intradermal nanoparticle delivery: potential for enhanced local administration of hydrophobic pre-formed photosensitisers. *Photodiagnosis Photodyn Ther* 7:222–231
- Elizabeth Fonseca dos Reis, Campos FS, Lage AP, Leite RC, Heneine LG, Vasconcelos WL, Lobato ZIP, Mansur HS (2006) Synthesis and characterization of poly (Vinyl Alcohol) hydrogels and hybrids for rMPP70 protein adsorption. *Mater Res* 9(2):185–191
- Egger NG, Schoenecker JA Jr, Gourley WK, Motamedi M, Anderson KE, Weinman SA (1997) Photosensitization of experimental hepatocellular carcinoma with protoporphyrin synthesized from administered delta-aminolevulinic acid: studies with cultured cells and implanted tumors. *J Hepatol* 26.4:913–920
- Fadel M, Kassab K, Fadeel DA (2010) Zinc phthalocyanine-loaded PLGA biodegradable nanoparticles for photodynamic therapy in tumor-bearing mice. *Lasers Med Sci* 25(2):283–292
- Ferrari M (2005) Cancer nanotechnology: opportunities and challenges. *Nat Rev Cancer* 5:161–171
- Gupta KC, Jabrail FH (2006) Effects of degree of deacetylation and cross-linking on physical characteristics, swelling and release behavior of chitosan microspheres. *Carbohydr Polym* 66:43–54
- Issa MC, Manela-Azulay M (2010) Photodynamic therapy: a review of the literature and image documentation. *An Bras Dermatol* 85(4):501–511
- Jain RA (2000) The manufacturing techniques of various drug loaded biodegradable poly(lactide-co-glycolide) (PLGA) devices. *Biomaterials* 21:2475–2490
- Jawahar N, Eagappanath T, Venkatesh N, Jubie S, Samanta MK (2009) Preparation and characterisation of PLGA-nanoparticles containing an anti-hypertensive agent. *Int J Pharm Tech Res* 1(2):390–393
- Jiang XY, Zhou CS, Tang KW (2003) Preparation of PLA and PLGA nanoparticles by binary organic solvent diffusion method. *J Central South Univ Technol* 10(3):202–206
- Kader A, Davis PJ, Kara M, Liu H (1998) Drug targeting using low density lipoprotein (LDL): physicochemical factors affecting drug loading into LDL particles. *J Control Release* 55:231–243
- Konan YN, Gurny R, Allemann E (2002) State of the art in the delivery of photosensitizers for photodynamic therapy. *J Photochem Photobiol B* 66(2):89–106
- Lamprecht A, Ubrich N, Hombreiro Perez M, Lehr C, Hoffman M, Maincent P (1999) Biodegradable monodispersed nanoparticles prepared by pressure homogenization-emulsification. *Int J Pharm* 184.1:97–105
- Lee SJ, Jeong JR, Shin SC, Kim JC, Chang YH, Chang YM, Kim JD (2004) Nanoparticles of magnetic ferric oxides encapsulated with poly (d,l lactide-co-glycolide) and their applications to magnetic resonance imaging contrast agent. *J Magn Magn Mater* 272:2432–2433
- Lee DJ, Park GY, Oh KT, Oh NM, Kwag DS, Youn YS, Oh YT, Park JW, Lee ES (2012) Multifunctional poly (lactide-co-glycolide) nanoparticles for luminescence/magnetic resonance imaging and photodynamic therapy. *Int J Pharm* 434(1–2):257–263
- Mansur HS, Sadahira CM, Souza AN, Mansur AAP (2008) FTIR spectroscopy characterization of poly (vinyl alcohol) hydrogel with different hydrolysis degree and chemically cross linked with glutaraldehyde. *Mater Sci Eng* 28(4): 539–548
- Murakami H, Kobayashi M, Takeuchi H, Kawashima Y (1999) Preparation of poly(DL-lactide-co-glycolide) nanoparticles by modified spontaneous emulsification solvent diffusion method. *Int J Pharm* 187(2):143–152
- Nah J, Jeong Y, Koh J (2000) Drug release from nanoparticles of poly(DL-lactide-co-glycolide). *Korean L Chem Eng* 17(2): 230–236
- Oh NM, Kwag DS, Oh KT, Youn YS, Lee ES (2012) Electrostatic charge conversion processes in engineered tumor-identifying polypeptides for targeted chemotherapy. *Biomaterials* 33:1884–1893

- Park SY, Baik HJ, Oh YT, Oh KT, Youn YS, Lee ES (2011) A smart polysaccharide/drug conjugate for photodynamic therapy. *Angew Chem Int Ed Engl* 50:1644–1647
- Qian X, Peng XH, Ansari DO, Yin-Goen Q, Chen GZ, Shin DM, Yang L, Young AN, Wang MD, Nie S (2008) In vivo tumor targeting and spectroscopic detection with surface-enhanced Raman nanoparticle tags. *Nat Biotechnol* 26:83–90
- Saxena V (2005) Development of polymeric nanoparticle delivery system for indocyanine green. PhD thesis submitted to the faculty of Graduate Division, College of Pharmacy and Allied Health Professions, Saint John University, Jamaica
- Tang T, Zheng J, Chen B, Li H, Li X, Xue K, Ai X, Zou S (2007) Effects of targeting magnetic drug nanoparticles on human cholangiocarcinoma xenografts in nude mice. *Hepatobiliary Pancreat Dis Int* 6:303–307
- Thakkar H, Sharma RK, Mishra AK, Chuttani K, Murthy RSR (2004) Efficacy of chitosan microspheres for controlled intra-articular delivery of celecoxib in inflamed joints. *JPP* 56:1091–1099
- Venslauskas MS, Batiuskaite D (2003) Irregular solid tumor growth: estimation of electrochemotherapy efficacy. *Acta Med Lituanica* 10:28–32
- Wu L, Zhang J, Watanabe W (2011) Physical and chemical stability of drug nanoparticles. *Adv Drug Deliv Rev* 63(6):456–469
- Yoo JJ, Kim C, Chung CW, Jeong Y, Kang DH (2012) 5-aminolevulinic acid-incorporated poly(vinyl alcohol) nanofiber-coated metal stent for application in photodynamic therapy. *Int J Nanomed* 7:1997–2005
- Zeng QB, Sun M (2009) Poly (lactide-co-glycolide) nanoparticles as carriers for norcantharidin. *Mater Sci Eng C* 29(3):708–713
- Zhang N, Chittasupho C, Duangrat C, Siahaan TJ, Berkland C (2007) PLGA nanoparticle-peptide conjugate effectively targets intercellular cell-adhesion molecule-1. *Bioconjug Chem* 19:145–152